CONFERENCE PRE-PRINT

STUDY ON THE KEY TECHNOLOGIES INVOLVED IN THE LASER NEUTRALISATION OF NEGATIVE ION SOURCE

HONG, H.H. ^{ab}, LIANG, L.Z. ^a, WANG, Q.X. ^{ab}, LI, B. ^{ab}, WANG, F. ^{ab}, YUN, Y. ^{ab}, XIE, H.R. ^{ab}, XIE, Y.L. ^{a*} a Institute of Plasma Physics, Hefei Institutes of Physical Science, Chinese Academy of Sciences Hefei, China

b University of Science and Technology of China Hefei, China

*Email: laurrence@ipp.ac.cn

Abstract

Neutral beam injection is one of the most effective auxiliary heating methods for magnetic confinement fusion. The traditional gas-target method has inherent drawbacks. For example, the neutralization efficiency is limited to 60% and decreases with the increase of beam energy. Moreover, the increase in gas-target thickness poses a significant challenge to the vacuum system. In contrast, laser neutralization can theoretically achieve a neutralization efficiency of over 90%. However, it has not been applied to practical devices so far due to the difficulty in maintaining long-term stable operation of high-power laser cavities at the MW level. Based on the parameterization factor calculation of laser neutralization efficiency and the layout of the negative ion beam transport system, the paper presents a detailed design and calculation of a triangular folded resonant laser cavity. Combining with the paraxial optical transmission matrix, the key parameters of the cavity topology, including the incident angle θ , the cavity mirror curvature R, the cavity length L, and the spot size w(z) along the optical path, are theoretically analyzed and obtained. The calculation method and results can be extended to resonant ring cavities with more folding times and larger sizes, which can be used to quickly determine the laser cavity structure required for the input conditions of the ion beam.

1. INTRODUCTION

Neutral beam injection (NBI) is a widely used effective method for plasma heating, current drive, and diagnostics in magnetic confinement fusion (MCF) experiments. The ITER design considers at least two neutral beams with 1 MeV@20 MW, using negative ions (H- or D-) as the particle source [1, 2]. The DEMO project is also considering the role of NBI in fusion power generation [3, 4]. The key sources of efficiency loss in NBI systems include ion beam generation, acceleration, and neutralization processes. Negative ion beams are preferred for high-energy neutral beam injection because they can effectively overcome the decrease in neutralization efficiency of positive ion beams with increasing beam energy. The neutralization process of negative ion beams includes metal vapor targets, gas targets, plasma targets, and laser targets [5-12]. Gas targets are currently the mainstream neutralization method. They work by injecting background gas of the same species to collide with the negative ion beam, converting it into a neutral atom beam while producing various particle components. This method is simple and effective but has inherent drawbacks. The maximum neutralization efficiency of gas targets is 60%, which does not meet the efficiency requirements of future fusion power generation devices for auxiliary heating systems. Additionally, increasing the gas target thickness poses a significant challenge to the vacuum system [5]. Laser neutralization involves using a laser beam of specific energy to strip the weakly bound electrons from the negative ion beam, producing neutral atoms without ionizing them and without introducing new ion or molecular species. Theoretically, the neutralization efficiency can reach 63% in a single collision and over 95% with three overlapping interactions. This process does not increase gas load, does not cause beam divergence, and simplifies the design of the residual ion deflection and recovery system. Every coin has two sides. The photonnegative ion collision cross-section is extremely small (10⁻²¹ m²), which necessitates extremely high laser power. For example, the saturation laser power for a 100 keV H⁻ ion beam is approximately 5 MW. Long-pulse operation of high-power lasers can cause significant photothermal effects on mirrors, limiting the linear increase of the cavity enhancement factor and causing component damage potentially. Moreover, the interaction volume increases with the thickness of the laser target, posing a significant challenge to system stability.

As a core component of the laser system, the structure of the enhancement cavity plays a decisive role in the output and distribution of laser intensity. External resonator technology involves selecting cavity parameters in the interaction zone to build a resonator, coupling the fundamental laser into the resonator, and using frequency locking technology to resonate it within the cavity. This effectively increases the incident laser power and achieves passive coherent amplification. In 2015, the Italian team designed a pulsed laser ring cavity based on second-

harmonic generation (SHG) technology, which significantly increased the laser power within the cavity. However, this approach increased the difficulty of incident laser pumping power and beam fine-tuning, and also increased the thermo-mechanical instability of the entire cavity [13, 14]. In 2018, the Russian team designed an Adiabatic trap cavity. Experimental results showed that the incident laser power was amplified to 2.1 kW and confined within the trap. For H⁻ and D⁻ beams below 10 keV, the maximum neutralization efficiency reached 95%, but this cavity type is entirely dependent on mirrors, with very high requirements for reflectivity and surface defects [15]. In 2018, the French team used a fiber laser to build a passive three-mirror ring cavity with F=3700 and Q=900, with a total cavity length of 1 m and a beam waist of about 700 µm, achieving over 50% neutralization on a 1.2 keV H⁻ beam [16]. For laser neutralization, directly feeding MW-level lasers to interact with high-energy ion beams is impractical. Considering the parametric factors affecting neutralization efficiency, folded resonant ring cavities have become the mainstream research focus.

Aiming to meet the requirements of laser neutralization for the optical cavity, including cavity stability, spot size in the interaction zone, and intracavity laser power, the paper systematically analyzes the laser transmission characteristics and the core parameters of the optical path structure of the triangular ring cavity based on the paraxial optical transmission matrix. The numerical calculation results can be used to quickly calculate and flexibly adjust the cavity configuration required for laser neutralization. The results and methods presented in the paper can be extended to resonant ring cavities with more folding times and larger sizes, laying a theoretical foundation for tabletop experiments and practical laser neutralization systems.

2. CAVITY PARAMETER ANALYSIS AND DESIGN

Taking the incident mirror M1 as the reference plane, a cyclic transmission matrix M_{rt} applicable to any open cavity is constructed, as shown in Equation (1). The triangular ring cavity is a symmetric cavity. Based on geometric relationships, the core configuration parameters of the cavity structure can be obtained as (θ_1, L_1, R_3) . Here, θ_1 represents the incident angle, L_1 denotes the distance between two reflective mirrors, M_1 and M_2 are plane mirrors, and R_3 is the curvature radius of the curved mirror, as illustrated in Fig. 1.

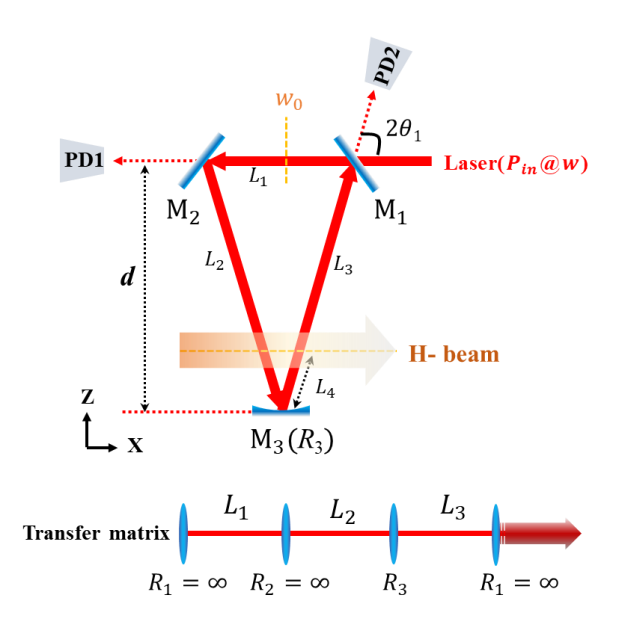


FIG. 1. Triangular ring optical path

$$M_n = \begin{pmatrix} A & B \\ C & D \end{pmatrix} = \begin{pmatrix} 1 & 0 \\ 0 & 1 \end{pmatrix} \begin{pmatrix} 1 & L_3 \\ 0 & 1 \end{pmatrix} \begin{pmatrix} 1 & 0 \\ -R_3/2 & 1 \end{pmatrix} \begin{pmatrix} 1 & L_2 \\ 0 & 1 \end{pmatrix} \begin{pmatrix} 1 & 0 \\ 0 & 1 \end{pmatrix} \begin{pmatrix} 1 & L_1 \\ 0 & 1 \end{pmatrix} (1)$$

$$I = \left[\frac{1}{2}(A+D)\right]^2 < 1(2)$$

Assuming $\theta_1 \in (22.5^{\circ} \rightarrow 45^{\circ})$, the algebraic expression for the stability factor $I(L_1,R_3)$ can be derived. Further, by satisfying the stability condition—Equation (2)—the variation of I for different combinations of L_1 and R_3 can be obtained, as shown in Fig. 2.

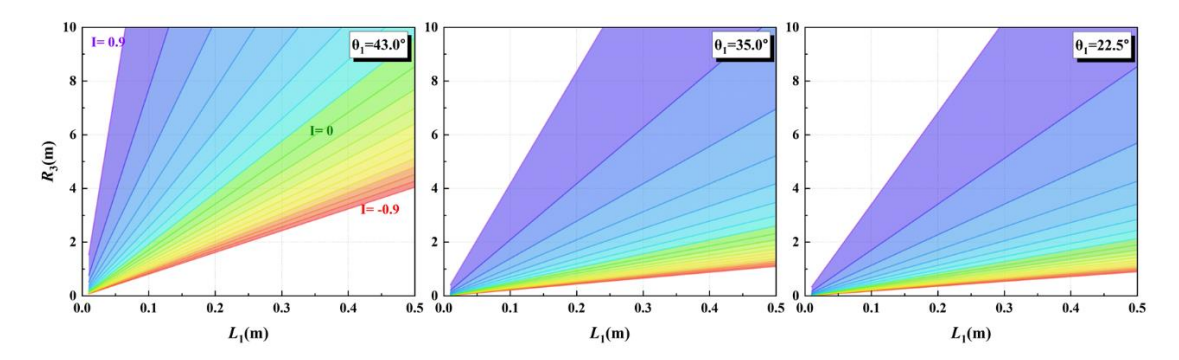


FIG. 2. Relationship between I, L1, and R3 for fixed $\theta 1$ =22.5°, 35° and 43°

Each region in the Fig. 2 represents a different combination of (L_1, R_3, I) . The colored regions indicate stable cavity parameters (θ_1, L_1, R_3) with varying values of I. As I increases from -1 to 1, the slope also increases, indicating greater sensitivity to changes in (L_1, R_3) . Specifically, when R_3 is fixed and L_1 is increased, the stability factor I approaches -1. Similarly, when L_1 is fixed and R_3 is decreased, I also approaches -1. Therefore, parameter values corresponding to $I \rightarrow -1$ should be prioritized. In practical optical path experiments, it is easier to adjust the relative distance L_1 after fixing the mirror M_3 . Therefore, by fixing (θ_1, R_3) at a specific value, the laser parameters at any position along the optical path can be obtained using the transmission matrix M (θ_1, L_1, R_3) , as shown in Fig. 3.

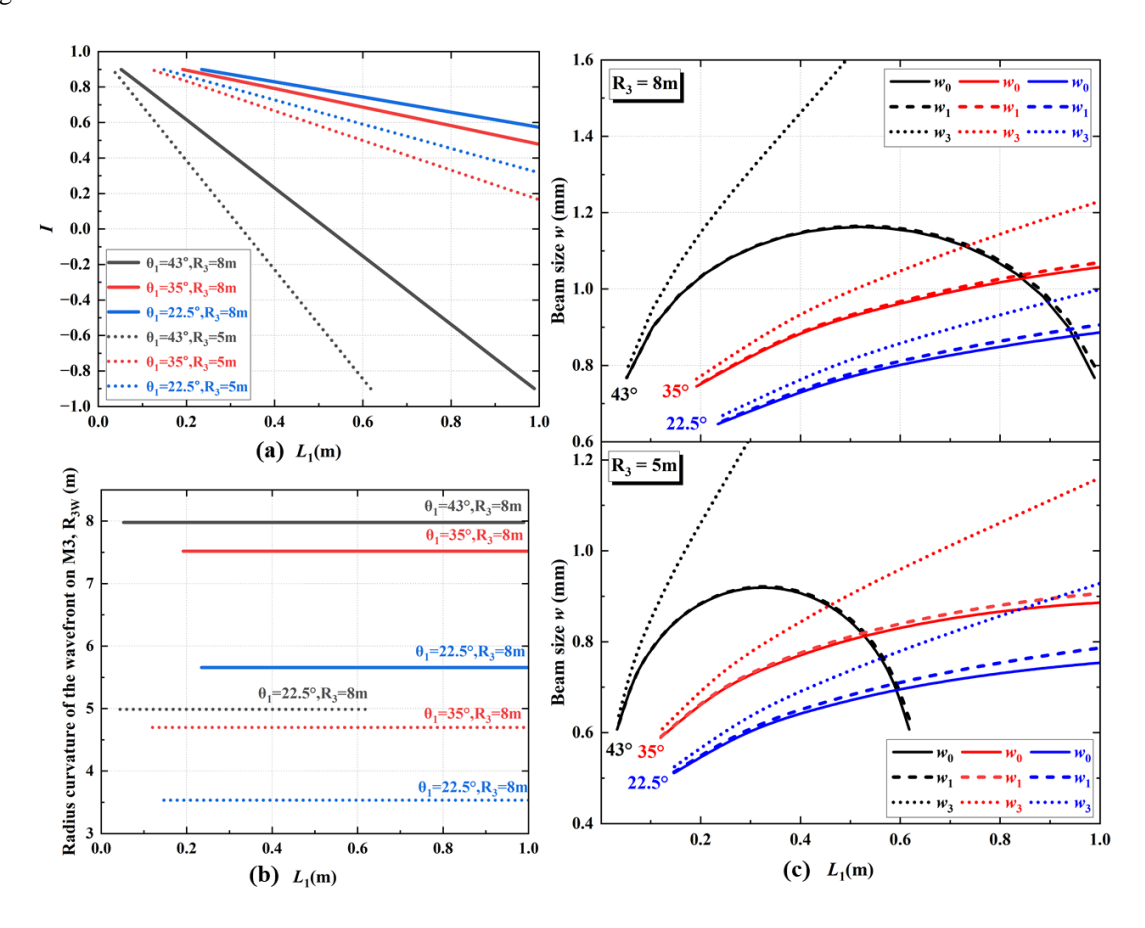


FIG. 3. For fixed values of $\theta_1 = (22.5^{\circ}, 35^{\circ}, 43^{\circ})$ and $R_3 = (6m, 8m)$, the variation of (a) the stability factor I, (b) the curvature radius of laser wavefront on mirror M_3 (R_{3W}), and (c) the spot size w with L_1

As shown in Fig. 3 (a) and (b), as the incident angle θ_1 approaches 45°, the stability factor I can quickly approach -1 with the variation of L_1 , and the radius of curvature of the wavefront on mirror M_3 also approaches the set value of R_3 , indicating that the laser cavity can more easily achieve a stable state. The distance $L_2=L_3$ also increases with the increase of θ_1 , which is beneficial for the mirrors to be farther away from the sputtering contamination of the high-energy ion beam. It can also be seen from Fig. 3 (a) and (b) that the effective range of (L_1, L_3) increases with the increase of R_3 . Fig. 3 (c) shows the variation of the spot sizes w_1 and w_3 on mirrors w_1 and w_2 , so the difference between w_1 and the waist value w_0 with w_1 . The waist of the triangular ring cavity is between w_1 and w_2 , so the difference between w_1 and the waist w_0 is very small. When (θ_1, R_3) is determined, with the increase of w_1 , both w_2 and the waist w_3 first increase and then decrease, while w_3 is always greater than w_1 and the waist w_2 while increasing. Under the same conditions, increasing w_1 and w_2 is conducive to increasing the spot size w_1 are various locations along the optical path. If w_1 is further determined, the specific spot size for interaction with the ion beam can be obtained based on the laser transmission within the cavity, and thus the theoretical value of the neutralization efficiency can be calculated.

Based on the parameter patterns shown in Fig. 2 and 3, specific values for (I, θ_1, L_1, R_3) can be obtained, which in turn determine the optical path configuration and enable the construction of the optical path, as shown in Fig. 4. The interaction zone represented by the optical cavity is placed inside a vacuum chamber. The seed light from the oscillator, after being regulated, amplified, and collimated, is optimized for mode matching by the lens group (f_1, f_2) and is ultimately transmitted into the cavity via mirror M_1 . PD2 receives the reflected laser from M_1 and the transmitted laser after laser circulation, which allows for the measurement of the transient coupling ratio of the incident laser entering the cavity. The PDH servo optical path locks the error signal generated, and the PZT regulates the seed laser, ensuring that the incident laser repetition rate is locked to free spectral range of the cavity, achieving stable cavity resonance. The transmitted laser after M_2 is split by a beam splitter, with portions received by PD1 and a beam spot profiler, respectively, to obtain the intracavity laser power and beam spot size. The cavity finesse F and power enhancement factor can also be measured using the laser power attenuation curves from PD1 and PD2.

By simultaneously adjusting $(L_1, R_3) \times \alpha$, the size of the three-mirror ring cavity and the spot size along the optical path can be scaled while maintaining the stability factor I constant. It should be noted that although a larger R_3 provides a wider adjustable range for L_1 and L_2 , which is beneficial for practical laser neutralization devices, it is not reasonable for actual tabletop optical path construction. If the goal is merely to reduce the cavity size, θ_1 can be decreased to obtain a suitable size for (L_1, L_2) . However, decreasing θ_1 makes the realization of the self-mode more difficult. Therefore, a comprehensive consideration of the core parameters (θ_1, L_1, R_3) is necessary to select an appropriate three-mirror ring cavity for experimentation and assembly.

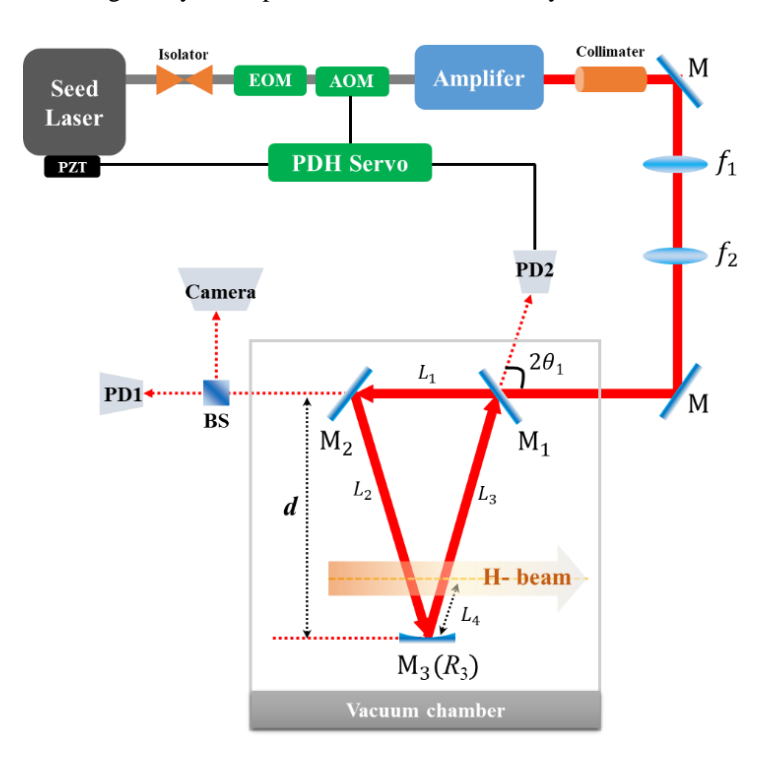


FIG. 4. Schematic diagram of the tabletop experimental optical path.

3. CONCLUSIONS

In a steady-state scenario, the NBI system must provide sufficiently high neutralization efficiency and electrooptical conversion efficiency. Since its inception, laser neutralization has garnered significant attention in the NBI
domain. Based on the physics of photo-detachment, research on laser neutralization primarily focuses on highpower lasers, high-gain cavities, and laser-negative ion interaction and separation. The impracticality of directly
feeding high-power lasers has made high-gain folded cavities the current research focus and a potential
breakthrough for practical applications in laser neutralization. Considering the parametric factors affecting laser
neutralization efficiency, the paper takes a triangular folded resonant cavity as an example and provides a detailed
analysis of the laser transmission characteristics of the ring cavity. Using matrix optics calculations, the core
parameters of the optical path structure can be obtained, including the incident angle θ_1 , mirror curvature R, cavity
length L, and spot size w(z) at various locations along the optical path. Additionally, we present a schematic
diagram of the optical path for practical experiments. The results and patterns obtained in the paper can be used
to flexibly adjust the cavity structure during tabletop experiments and to calculate the cavity structure required for
the layout of negative ion source beamlines quickly.

The power enhancement factor of the cavity is another crucial parameter for laser neutralization. It is gradually reduced due to thermal effects and, in a steady state, depends on the reflectivity of the mirrors and cavity losses, which are not discussed in the paper. In the subsequent phase of research, we will concentrate on integrating the construction of the optical path with experimental outcomes, thereby conducting a comprehensive and in-depth investigation into this particular aspect.

ACKNOWLEDGEMENTS

This work was supported by Comprehensive Research Facility for Fusion Technology Program of China under Contract No. 2018-000052-73-01-001228.

REFERENCES

- [1] TOIGO, V., BOILSON, D., BONICELLI, T., et al., Progress in the realization of the PRIMA neutral beam test facility, Nucl. Fusion 55 (2015) 083025. https://doi.org/10.1088/0029-5515/55/8/083025
- [2] TOIGO, V., BELLO, S.D., BIGI, M., et al., Progress in the ITER neutral beam test facility, Nucl. Fusion 59 (2019). https://doi.org/10.1088/1741-4326/ab2271
- [3] SONATO, P., AGOSTINETTI, P., BOLZONELLA, T., et al., Conceptual design of the DEMO neutral beam injectors: Main developments and R&D achievements, Nucl. Fusion 57 (2017) 056026. https://doi.org/10.1088/1741-4326/aa6186
- [4] TRAN, M.Q., AGOSTINETTI, P., AIELLO, G., et al., Status and future development of Heating and Current Drive for the EU DEMO, Fusion Eng. Des. (2022). https://doi.org/10.1016/j.fusengdes.2022.113159
- [5] SARTORI, E., PIMAZZONI, A., VELTRI, P., et al., "Improving the Transported Negative Ion Beam Current in NIO1", Proc. Int. Symp. Neg. Ions, Beams and Sources (2018). https://doi.org/10.1063/1.5083782
- [6] GRISHAM, L.R., Lithium Jet Neutralizer to Improve Negative Ion Neutral Beam Performance, Am. Inst. Phys. (2009). https://doi.org/10.1063/1.3112533
- [7] HANADA, M., KASHIWAGI, M., INOUE, T., et al., Experimental comparison between plasma and gas neutralization of high-energy negative ion beams, Rev. Sci. Instrum. 75 (2004) 1813–1815. https://doi.org/10.1063/1.1699462
- [8] SURREY, E., Gas heating in the neutralizer of the ITER neutral beam injection systems, Nucl. Fusion 46 (2006) S360. https://doi.org/10.1088/0029-5515/46/6/S18
- [9] DONATELLA, F., ALESSANDRO, F., Overview of photo-neutralization techniques for negative ion-based neutral beam injectors in future fusion reactors, Eur. Phys. J. D. At. Mol. Opt. Phys. (2022). https://doi.org/10.1140/epjd/s10053-022-00457-9
- [10] O'CONNOR, A.P., GRUSSIE, F., BRUHNS, H., et al., Generation of neutral atomic beams utilizing photodetachment by high power diode laser stacks, Rev. Sci. Instrum. 86 (2015) 113306. https://doi.org/10.1063/1.4934873
- [11] SIMONIN, A., ACHARD, J., ACHKASOV, K., et al., R&D around a photoneutralizer-based NBI system (Siphore) in view of a DEMO Tokamak steady state fusion reactor, Nucl. Fusion 55 (2015) 123020. https://doi.org/10.1088/0029-5515/55/12/123020
- [12] HEMSWORTH, R.S., VELTRI, P., Design of a Plasma neutraliser for a Fusion reactor or as an upgrade to the ITER heating neutral beam injectors, Fusion Eng. Des. 202 (2024). https://doi.org/10.1016/j.fusengdes.2024.114322
- [13] VINCENZI, P., FASSINA, A., GIUDICOTTI, L., et al., Design and mockup tests of the RING photo-neutralizer optical cavity for DEMO NBI, Fusion Eng. Des. (2019). https://doi.org/10.1016/j.fusengdes.2019.02.076
- [14] FASSINA, A., FIORUCCI, D., GIUDICOTTI, L., et al., Performance analysis and application study of a laser enhancement cavity for photo-neutralization of Negative Ion Beams, J. Instrum. (2020)
- [15] POPOV, S.S., ATLUKHANOV, M.G., BURDAKOV, A.V., et al., Neutralization of negative hydrogen and deuterium ion beams using non-resonance adiabatic photon trap, Nucl. Fusion 58 (2018) 096016.1–096016.9. https://doi.org/10.1088/1741-4326/aacb02
- [16] BRESTEAU, D., BLONDEL, C., DRAG, C., Saturation of the photoneutralization of a H⁻ beam in continuous operation, Rev. Sci. Instrum. 88 (2017) 113103. https://doi.org/10.1063/1.4995390